Life history adaptations to fluctuating environments: Combined effects of demographic buffering and lability of vital rates

Christie Le Coeur*[1], Nigel G. Yoccoz[2], Roberto Salguero-Gómez[3], and Yngvild Vindenes[1]

[1]Centre for Ecological and Evolutionary Synthesis (CEES), Department of Biosciences, University of Oslo, Norway

[2]Department of Arctic and Marine Biology, Faculty of Biosciences, Fisheries and Economics, UiT The Arctic University of Norway, Tromso, Norway

[3]Department of Zoology, University of Oxford, 11a Mansfield Rd, Oxford OX1 3SZ, UK

*Corresponding author: christielecoeur@gmail.com

Abstract

Demographic buffering and lability have both been identified as important adaptive strategies to optimise long-term fitness in variable environments. These strategies are not mutually exclusive, however we lack efficient methods to measure their relative importance. Here, we define a new index to measure the total lability for a given life history, and use stochastic simulations to disentangle relative fitness effects of buffering and lability. The simulations use 81 animal matrix population models, and different scenarios to explore how the strategies vary across life histories. The highest potential for adaptive demographic lability was found for short- to intermediately long-lived species, while demographic buffering was the main response in slow-living species. This study suggests that faster-living species are more responsive to environmental variability, both for positive or negative effects. Our methods and results provide a more comprehensive view of adaptations to variability, of high relevance to predict species responses to climate change.

Keywords: comparative study, convexity, demographic buffering, demographic lability, environmental variance, climate change, matrix population model, non-linearity, temporal covariance, stochasticity

Introduction

Understanding life history adaptations to fluctuating environments is increasingly important, as anthropogenic climate change is altering the temporal variability of multiple climatic drivers (IPCC, 2021; Laufkötter *et al.*, 2020; Pendergrass *et al.*, 2017). For instance, while an increased variance in daily and seasonal temperature and precipitation is expected across much of Europe in summer, a decrease is projected in other regions (Huntingford *et al.*, 2013; IPCC, 2021; Kotz *et al.*, 2021; Pendergrass *et al.*, 2017). Depending on the habitat, fluctuations in abiotic and biotic environmental drivers experienced by organisms may affect their relative fitness and select for specific adaptations to live in variable environments.

Two main mechanisms have been identified for adaptations to environmental variability, optimizing long-term fitness: Demographic buffering reduces the variance in vital rates (e.g., survival, fecundity), thereby minimizing the effects of bad environments, while demographic lability lets the organisms take advantage of good environments by mounting a large increase in some vital rates compared to an average or bad environment, and therefore increasing the mean of these vital rates (see Box 1 for Glossary). The two mechanisms are not mutually exclusive, as different vital rates of a given life history can show different responses to an environmental driver. Yet, these mechanisms have often been investigated separately, and we lack efficient methods to disentangle and predict their relative importance for a given life history and environment. Understanding how organisms combine lability and buffering of their different vital rates requires a demographic model framework to predict the net effects of non-linearity in responses of all vital rates to variability, as well as effects of covariation between the vital rates. While the latter is well described in stochastic demographic theory, we know much less about the impacts of non-linearity, representing the potential for adaptation through lability.

A key prediction from classical theory for evolutionary bet-hedging and stochastic population growth is that the long-term mean fitness will be reduced if the temporal variance of fitness

is increased (Lewontin & Cohen, 1969). This result is assuming an unstructured population with annual population growth rates that are IID (independently and identically distributed). The long-term fitness is then the logarithm of the geometric mean of these growth rates (Lewontin & Cohen, 1969). In structured populations, the stochastic growth process is more complex due to fluctuations in the (st)age structure that introduce autocorrelation in the annual growth rates (Caswell, 2001). Still, under the assumption of small fluctuations in the vital rates, Tuljapurkar (1982) derived an important approximation of long-term growth rate in stage-structured populations, emphasising how the variance in fitness is linked to variances and covariances of vital rates in different stages (Box 2). The key conclusion from this approximation is that temporal variability in vital rates will have a negative effect on long-term fitness, and should be selected against, in particular for vital rates that have a large impact on fitness in the mean environment. Accordingly, the demographic buffering hypothesis predicts that natural selection should favour a reduction in variance of the vital rates with the strongest influence on population growth (Boyce *et al.*, 2006; Hilde *et al.*, 2020; Koons *et al.*, 2009; Pfister, 1998; Tuljapurkar & Orzack, 1980).

However, positive effects of environmental variability have also been demonstrated under strong negative covariance among vital rates (Colchero *et al.*, 2019; Doak *et al.*, 2005; Tuljapurkar, 1990), negative environmental autocorrelation (also considered by Tuljapurkar (1982)), and convex relationships between vital rates and the environment. The latter represents a case of adaptive lability as described by Koons *et al.* (2009). In an unstructured population, a non-linear relationship between the environment and logarithm of the annual growth rate has straightforward impacts on how the environmental variance alters the long-term mean fitness: A convex relationship leads to positive variance effects, a concave relationship to negative variance effects, and linear relationships imply no effects of the variance (Drake, 2005; Ruel & Ayres, 1999). But with more complex, structured life histories the combined effects of nonlinearity in different vital rates on long-term fitness are more challenging to predict. In contrast to adap-

tive demographic buffering, which optimizes long-term fitness by reducing the variance of most influential vital rates, adaptive lability works by increasing the arithmetic mean of the annual growth rates through increased vital rate means (Box 1). Nonlinearity in vital rate and population responses may be common in the wild (Barraquand & Yoccoz, 2013; Clark & Luis, 2020; Dahlgren *et al.*, 2011; Drake, 2005; Hansen *et al.*, 2021; Jenouvrier *et al.*, 2012; Lawson *et al.*, 2015; Louthan & Morris, 2021; Mysterud *et al.*, 2001), highlighting the potential importance of lability as an adaptation to environmental variability.

Yet somewhat contrasting predictions have been made as to which vital rates should be labile or buffered, and the relative importance of each mechanism for a given life history. Demographic lability has been suggested to affect mainly the least influential vital rates, with low effect on average fitness (Hilde *et al.*, 2020), and occurring mainly concurrently with selection for buffering of more influential vital rates. Other studies suggest that lability can be equally important to demographic buffering, and that it can also occur in highly influential vital rates (Jongejans *et al.*, 2010; Koons *et al.*, 2009; McDonald *et al.*, 2017). Based on the latter prediction, recent research suggests that adaptive lability and buffering can be located at the opposite ends of a continuum, encompassing a wide range of demographic strategies (Salguero-Gómez, 2021; Santos *et al.*, 2021). Yet, the extent to which lability among the least or the most influential vital rates can be adaptive strategies for coping with varying environments, relative to buffering, remains largely unexplored (e.g., Barraquand & Yoccoz (2013)).

We thus need a more thorough understanding of how the opportunity for selection on demographic buffering and lability depends on major axes of life history variation such as the slow-fast continuum (Stearns, 1992; Gaillard *et al.*, 2016; Salguero-Gómez *et al.*, 2016b). For instance, populations of fast-living species have been predicted to be more responsive to increased environmental variability than those of slow-living species, and to be more likely to show adaptive lability in their vital rates (Dalgleish *et al.*, 2010; Iles *et al.*, 2019; Koons *et al.*, 2009; Morris *et al.*, 2008). According to the demographic buffering hypothesis theory, species

towards the slow end of the continuum benefit most from reduced variance in annual survival of the reproductive stages, while fast-living species gain relatively more from reduction of variance in annual fertility and/or survival of the non-reproductive stages (Hilde *et al.*, 2020; Gaillard & Yoccoz, 2003; Rotella *et al.*, 2012). These effects can be predicted from Tuljapurkar's small noise approximation (Tuljapurkar (1982); Box 2), but we lack a similar expression to describe the net impact of non-linearity in different vital rates of the same life history. Here, we introduce a new 'demographic lability index' to predict changes in the arithmetic mean arising from non-linearity in different vital rate responses to an explicit environmental driver. We test the precision of this index using stochastic simulations. We also investigate the opportunity of organisms to combine adaptive responses of buffering and lability depending on generation time, which closely correlates with the species' position along the slow-fast continuum (Gaillard *et al.*, 2005). We use population models from the COMADRE animal matrix database (Salguero-Gómez *et al.*, 2016a) as a starting point for our simulations, representing the life history in the constant environment. We then add stochastic variation and perform the simulations under different scenarios for non-linearity and covariance among vital rates (Fig. 1). To disentangle the contribution of vital rate curvatures (convex, concave, flat) to an environmental driver from vital rate variance and covariance, we decomposed the effect of environmental variability on long-term fitness into changes in the arithmetic mean fitness and variance. Our study addresses two main questions. First, what is the opportunity for positive effects due to adaptive lability to overcome negative impacts through the variance and covariance of vital rates (leading to an overall increased fitness in variable environments), and how does this pattern depend on generation time? Second, are vital rates that show adaptive lability typically the least or most influential vital rates?

Material and methods

To explore fitness responses to increased environmental variability along the slow-fast continuum, we used a simulation approach. The main response is the stochastic long-term population growth rate $ln(\lambda_s)$, which is a measure of long-term fitness (Fig. 1A) (Caswell, 2001; Lande *et al.*, 2003; Tuljapurkar, 1990). We defined nonlinear functions relating vital rates to an explicit environmental driver z (details below), and tested how the type and curvature of nonlinear vital rate functions, and the covariance structure between these rates affect $ln(\lambda_s)$ (Fig. 1A-C). To confront hypotheses about demographic lability, we specifically tested effects of lability among the vital rates expected to contribute the most or the least to population growth, keeping other vital rates constant ('forced buffering', see scenarios, Fig. 1C). All simulations and calculations were performed in R, version 4.0.3 (R Core Team, 2020). R codes are provided in Supporting information 6.

Baseline models for a constant environment

As a baseline for the simulations (values at $z = 0$) we used age- and stage-structured matrix population models (MPMs) from the COMADRE Animal Matrix Database (v.4.20.5; Salguero-Gómez *et al.* (2016a)). Each MPM includes a projection matrix that summarises the (st)age-specific fertilities, transitions, and survival rates for a given time interval (see Fig. 1). We selected MPMs from unmanipulated and free-ranging populations, considering only 'mean' matrices (i.e., one matrix per population) with annual time steps. We also restricted the analysis to MPMs with a deterministic population growth rate λ_0 ranging from 0.9-1.1 to limit population extinction during simulations (see Supporting information 1 for complete description of selection criteria). Eighty-one MPMs were selected, describing two amphibian, 20 bird, two bony fish, 39 mammal, and 18 reptile populations, belonging to 65 species. Generation time was calculated as the mean age of parents at the stable (st)age distribution (i.e., stable growth;

Caswell (2001)) and ranged from 1.7 years (White-tailed ptarmigan, *Lagopus leucura*) to 61.2 years (Arrau turtle, *Podocnemis expansa*) in our dataset.

Simulation framework: nonlinear vital rate responses and environmental stochasticity

Nonlinear relationships - For each MPM we assume that both survival rates and fertility coefficients were functions of a main environmental driver z, assuming constant transition rates among stages (for stage-structured populations). The environment z was assumed to follow a standard normal distribution. The survival probability of stage j is denoted $s_j(z)$, while the fertility coefficient (offspring produced to next year) is denoted $f_j(z)$. These functions were defined for each scenario using link functions (log-log or logistic link for survival, for fertility we also tested a log link; fig 1A-B), where the parameters were defined so that $s_j(0)$ and $f_j(0)$ corresponded to the value from the MPM in COMADRE. For instance, with a log-log link function, the survival rates are defined as $s_j(z) = \exp(-\exp(-\beta_0 - \beta_{z_S} * z))$, where the parameter β_0 is defined as $\beta_0 = -\ln(-\ln(s_j(0)))$. The parameter β_{z_S} defines the strength of the environmental effect on $s_j(z)$, and thereby also the degree of variability (Fig. 1A). This parameter can be positive or negative, shifting the direction of the environmental effect. For fertility coefficients we used an extra parameter $MaxF$ to set the maximum in scenarios using a log-log link or a logistic link. We used $MaxF = M * f_j(0)$ with M = 2.5, so that the maximum fertility was set as a proportion of the fertility in the mean environment. β_{z_F} defines the strength of the environmental impact. A complete description including equations for all link functions is provided in Supporting Information 2, and results for different values of M are shown in Supporting information 3.

A key simplifying assumption in our simulations is that the survival rates of different (st)ages all have the same value of β_{z_S}, and similarly all fertility coefficients have the same β_{z_F}. This means that 1) the values for the mean environment $s_j(0)$ and $f_j(0)$, defined by the COMADRE

matrix, control the curvature of the vital rate functions around the mean environment (Fig.1A and Fig.S2), and 2) there is always positive covariance between survival rates of different (st)ages and between the fertilities of different (st)ages. These assumptions are biologically realistic if individuals of different (st)ages live in the same environment, and their survival and reproduction are affected similarly by a key driver. A range of other scenarios are also possible but not considered here, such as no covariance between the vital rates. While we always have positive covariance within survival and within fertilities of different (st)ages, we consider different scenarios of negative or positive covariance between survival and fertility, by adjusting the signs of β_{z_S} and β_{z_F}. In our simulations, β_{z_F} and β_{z_S} were set to 0.5 or 0.1 to simulate scenarios of high and low effects of environmental variability on the vital rates, respectively (Fig. 1A; more scenarios in Supporting information 4).

Scenarios - Simulations were run under 13 scenarios (Fig. 1C) varying 1) the type of link function defining $s_j(z)$ and $f_j(z)$, 2) the covariance between survival and fertility; negative or positive (scenarios 1-8), and by applying 3) special cases of forced buffering, turning off the effect of z for certain vital rates (scenarios 9-13). In the first eight scenarios, all vital rates were affected by z as described above. Regarding type of link function, four combinations were tested including logistic functions for all vital rates, log-log link functions for all vital rates, and two combinations of log-link for $f_j(z)$ with logistic or log-log link functions for $s_j(z)$. Each of these four combinations was tested using positive or negative covariance between survival and fertility (scenarios 1-8, Fig. 1). In the scenarios of demographic lability with forced buffering, either the $s_j(z)$ (scenarios 9-11) or the $f_j(z)$ (scenarios 12-13) were held constant and equal to their value in the mean environment as reported in the COMADRE projection matrix. Here we used logistic functions for the other vital rates (Fig. 1). These scenarios reflect different assumptions of demographic lability and buffering within the least or the most influential vital rates on population growth, depending on the position of the populations along the slow-fast continuum of life histories. According to theoretical expectations, survival of non-reproductive

stages and fertility were assumed to show a higher contribution to population growth of fast-living species while survival rates of the reproductive stages were assumed the most influential for slow life histories.

Stochastic perturbations - For each of the 13 scenarios and for each selected population, 4,000 simulated time series of population growth were generated, each representing 200 years. For each simulated year a value of the environment z was drawn from the standard normal distribution, and used to calculate the corresponding projection matrix, resulting in a time series of projection matrices. Starting from a population of 100 individuals, equally distributed among the (st)ages, we computed the stochastic population growth rate for each of the 4000 simulations as the average growth increment of the total reproductive value of the population ($V_t = \sum_{j=1}^{k} v_j n_{t,j}$, where v_j is the reproductive value of stage j and $n_{t,j}$ is the size of (st)age j at time t), using the estimator $ln\lambda_s = \frac{1}{200}\sum_{t=1}^{200} lnV_t - lnV_{t-1}$ (Engen *et al.*, 2009). We then took the average value from the 4000 simulations as the estimate for the given population and scenario. The reproductive values act as a filter for fluctuations in the (st)age structure, and remove biases due to the populations being further away from the stable structure in the beginning of simulations (Engen *et al.*, 2009).

For each scenario and population, we calculated the difference in $ln(\lambda_s)$ between the scenarios of high and low environmental variability, referred to as $\Delta ln(\lambda_s)$. The sign of this estimate indicates whether increased environmental variability has a positive ($\Delta ln(\lambda_s) > 0$) or negative ($\Delta ln(\lambda_s) < 0$) effect on the stochastic population growth rate. The larger the value (positive or negative), the larger is the effect of the environmental variance on long-term fitness.

Partitioning the effects of demographic lability and buffering on long-term fitness

As a starting point we considered Tuljapurkar's 'small-noise' approximation (Box 2). For each simulation run we decomposed the net effect of environmental variance on long-term fitness $\Delta ln(\lambda_s)$ into changes in the arithmetic mean $\Delta ln(\bar{\lambda})$, reflecting lability effects, and changes

in the variance of annual population growth rates $\Delta\sigma^2 = \Delta(\frac{\sigma^2_\lambda}{2\bar{\lambda}^2})$, reflecting buffering effects (Box 2). A positive $\Delta ln(\bar{\lambda})$ indicates that the overall effect of lability of vital rates is positive, and requires that some vital rates show convex relationships with the environmental driver (see next section). The value of $\Delta\sigma^2$ indicates the contribution of increased environmental variability through the variance of population growth caused by variance and covariance of the vital rates, and can be reduced through buffering.

A demographic lability index for life histories

To assess the net impact of vital rate curvatures on the direction and strength of the mean response $\Delta ln(\bar{\lambda})$, we defined the following demographic lability index (DLI):

$$\text{DLI} = \sum_{j=1}^{k} s''_j(0)\frac{d\lambda_0}{ds_j(0)} + f''_j(0)\frac{d\lambda_0}{df_j(0)}, \tag{1}$$

where the sum is over all stages, $s''_j(0)$ and $f''_j(0)$ denote the second derivatives of survival and fertility with respect to z, at the value $z = 0$ (first and second derivative expressions for each link function are provided in Supporting information 6). If the second derivative is positive, the vital rate function is convex at $z = 0$. The sensitivities measure the influence of each vital rate on λ_0 in the mean environment, and are used to weight the impact of the curvatures to estimate the total effect of lability. Thus, a vital rate with strong convex curvature may still have a low impact on the DLI if the corresponding sensitivity of λ_0 to that vital rate is low. The DLI is intended to capture the overall effect of lability and indicate whether it is positive (adaptive) or negative (not adaptive), and thus the effect on the mean response $\Delta \ln \bar{\lambda}$. The DLI was estimated for each population in the 13 scenarios for $\beta_{z_{0.5}}$ (Fig. 1A).

Results

Covariance structure and nonlinear vital rates

In all scenarios, life histories with short to intermediate generation times (< 10 years) showed consistently stronger responses to environmental variability than populations with slow life histories (Fig. 2-3). Whether these responses are positive or negative, strongly depends on the vital rate curvature and covariance structure between the (st)age-specific survival rates and fertility coefficients.

A positive DLI, indicating adaptive lability through overall positive contribution from convex vital rate responses, was reported mainly among the fast-living species (Fig. 2-3). This index correlated almost perfectly with change in $ln(\bar{\lambda})$ (Spearman coefficient > 0.98 in all scenarios), suggesting that this is a reliable indicator of adaptive lability. However, to predict the net effect on long-term fitness $ln(\lambda_s)$, effects through the variance-covariance of the vital rates must also be taken into account.

With positive covariance between survival and reproduction, environmental variance reduced $ln(\lambda_s)$ in the simulations, regardless of the value of the DLI and the type of vital rate functions used (e.g., log-log link and logistic functions in Fig. 2). This result confirms that the covariance structure is an important driver of population responses to environmental variability (Fig. 2-3). In these scenarios, $\Delta\sigma^2$ was on average more than 12 times higher than in corresponding scenarios using negative covariance (e.g. Fig. 2b VS fig. 2d). Increases in $ln(\bar{\lambda})$ could still occur, but was not sufficient to overcome the negative effect of the increased σ^2 that results from the positive covariance in vital rates. In contrast, populations of fast-living species could show an overall positive effect of increased environmental variability on long-term fitness if survival and fertility covaried negatively ($\Delta ln(\lambda_s) > 0$; Fig. 2c and 3), unless $s_j(z)$ and $f_j(z)$ were defined by log-log link functions (i.e., harsher relationships; Fig.2d). Positive effects were stronger when we used a log-link function for the fertility coefficients, so that it increased exponentially with

the environmental driver z leading to strong convexity (Fig. 3c-d).

Demographic lability with forced buffering

In these scenarios, some vital rates were kept constant and buffered, while others were allowed to vary. The identity of labile vital rates, together with the position of the species along the slow-fast continuum, affected the direction and strength of population responses to environmental variability (Fig. 4). In fast-living species, lability in all survival rates $s_j(z)$ or in only the mature stages $s_{mature}(z)$ combined with a constant fertility (Fig. 4a-b) led to a small increase of $ln(\lambda_s)$. This increase ($\Delta ln(\lambda_s) > 0$) correlated with a positive DLI, a corresponding positive $\Delta ln(\bar{\lambda})$, and a low $\Delta\sigma^2$. Positive effects of lability in fertility $f_j(z)$ and survival rates of the immature stages $s_{immature}(z)$, expected to be more influential in these fast populations, were also detected especially when these rates covaried negatively (Fig. 4c-e).

In contrast, for slow-living species, labile survival rates of the reproductive stages $s_{mature}(z)$ combined with constant fertility rates $f_j(z)$ and constant survival of immature stages $s_{immature}(z)$ (Fig. 4b; hypothesis of lability among the most influential vital rates) always produced a negative DLI and negative effects on $ln(\lambda_s)$. The scenario of lability in fertility coefficients combined with constant (st)age-specific survival rates strongly reduced σ^2 and caused a shift in the DLI from negative to zero, revealing low effect of variability on $ln(\bar{\lambda})$ ($\Delta ln(\bar{\lambda}) \approx 0$) and a weak positive effect on $ln(\lambda_s)$ (Fig. 4c). In other words, constant (st)age-specific survival rates associated with labile fertility coefficients have a stabilizing effect on $ln(\lambda_s)$ of slow life histories (generation time > 10 years; Fig. 4c VS Fig. 4a-b). The stochastic population growth rate of these species remained stable when both fertility rates and survival of immature stages were labile (Fig. 4d-e).

Discussion

This study emphasizes the importance of considering explicit links between environmental drivers and vital rates to understand the effects of environmental variability on long-term fitness. We provided a new index for predicting the net effect of lability in a given life history, complementing earlier theory focusing mainly on buffering. By disentangling the effects on the arithmetic mean and variance of the annual growth rates, we could measure the combined effects of demographic lability and buffering for a given life history, and compare them across life histories. Populations among the faster-living species were identified as the most responsive to increased environmental variance, both through changes in the mean and variance. Positive effects correlated with a positive DLI, and this index contributes to predict the overall response of long-term fitness, which also depends on the variance and covariance of vital rates. Here, a positive overall effect of environmental variability on long-term fitness was only found when a positive DLI was combined with negative covariance between survival and fertility. When combined with constant vital rates (forced buffering), lability in both the least and the most expected influential vital rates were found to benefit long-term fitness to some extent, but only for short-lived species. Our study provides a step forward in our understanding of fitness responses to environmental variability over a wide range of life histories and stresses the importance of characterising both curvatures and covariances of vital rates with respect to key drivers in order to understand life history adaptations as well as to predict population responses to increased variability under global change.

Fast life histories are more responsive to changes in environmental variability: positive and negative responses

Several studies have shown evidence that populations located at the fast end of the fast-slow continuum are more sensitive to changes in the different components of climate change. These

populations tend to respond more strongly to climate drivers (e.g., Compagnoni *et al.* (2021)), to changes in demographic or environmental variability (e.g., Dalgleish *et al.* (2010); Drake (2005); Koons *et al.* (2009); Morris *et al.* (2008), but see Le Coeur *et al.* (2021); Santos *et al.* (2021)), to shifts in temporal autocorrelation in the environment (e.g., Paniw *et al.* (2018)) and to shifts in vital rate correlations (Iles *et al.*, 2019). In line with these previous studies, we found that populations of faster-living species were more responsive to increased environmental variability compared to those of slow living-species. Increased variability in a main environmental driver can either benefit or adversely impact population fitness of these life histories. They can be more vulnerable due to higher variance in annual population growth rates on average (increased σ^2), as reported in previous studies (e.g., Dalgleish *et al.* (2010); Morris *et al.* (2008)); or conversely, they can benefit more from adaptive lability through convex vital rate responses (increased $ln(\bar{\lambda})$). A positive DLI correlated with an increase of $ln(\bar{\lambda})$ in our simulations, and led to positive overall effect on the stochastic population growth rates when associated with negative temporal covariance between fertility and survival rates.

A majority of studies have focused on effects on increased vital rate variance alone, without explicit reference to the underlying environmental drivers, even though other studies (Drake, 2005; Henden *et al.*, 2008; Koons *et al.*, 2009) highlighted the potentially critical importance of including such links. Our results support this conclusion, and show that the total effects of environmental variance on the dynamics of structured populations may be either positive or negative if nonlinear vital rate responses are present. With explicit links where some are convex, positive fitness responses are possible, but we highlight that the net effect depends on the covariance structure of vital rates and the type of link functions as well. Evidence of convex relationships between vital rates and key environmental drivers is still limited for natural populations, due to data limitation or *a priori* linear assumptions in the statistical models, and there is a need for empirical research to determine more systematically the shape and curvature of vital rate responses to accurately predict demographic responses to environmental variance.

Characterizing the relationships between environmental drivers and all vital rates remains, however, a statistical challenge for wild populations (e.g., separating link functions Gill (2001)) and requires long-term monitoring data. This highlights the need to continue and increase the ongoing collection of demographic data.

Role of temporal covariance between (st)age-specific vital rates

While negative covariance between vital rates could arise from life history trade-offs (Stearns, 1989) or opposite responses to the same environmental driver, positive covariances between vital rates are just as likely to occur in a population. For instance, good environmental conditions such as high resource availability, could enhance survival of different (st)ages in a population (e.g., juvenile and adult survival) or favour both juvenile survival and adult fertility. Theory suggests that positive and negative covariances amplify or weaken the temporal variability in annual population growth, respectively (Tuljapurkar, 1982,9), which in turn influence the stochastic population growth rate. Our results are in line with these predictions, showing reduced variance of the annual population growth when survival and fertility rates covaried negatively compared to positively. However, the consequence on $\ln(\lambda_s)$ for a given population is expected to be highly dependent on the magnitude of the covariance, the nature and curvature of the vital rates involved and their combined contribution to long-term fitness.

Interestingly, there is no general consensus on the degree to which positive or negative covariance in vital rates are more common in the wild, nor if the sign, magnitude or type of (st)age-specific vital rates involved correlate with the position of a species along the fast–slow continuum. From empirical studies, positive covariance have been reported predominantly in several long-lived species (e.g., Dahlgren *et al.* (2016); Rotella *et al.* (2012); van de Pol *et al.* (2010)) with substantial (e.g., Coulson *et al.* (2005)) or weak (e.g., Altwegg *et al.* (2007); Compagnoni *et al.* (2016); Johnson *et al.* (2010)) effects on long-term fitness. In contrast, negative covariance were less often detected, with often little effect on $\ln(\lambda_s)$. To our knowledge,

relatively few studies have specifically addressed this question among species towards the fast-end of the continuum.

In our scenarios, we assumed a perfect, positive temporal covariance between (st)age-specific survival rates and between (st)age-specific fertilities, respectively, but positive or negative covariances between survival and fertility. While these assumptions on the direction of covariance between stages and type of vital rates are plausible, they are strong in terms of magnitude, and a main environmental driver is unlikely to explain all of the (co)variance in vital rates. Our results may therefore overestimate the magnitude of the variance in population growth compared to wild populations where correlations are likely less perfect, especially for scenarios were all vital rates show positive covariance. Even though a strong covariance between vital rates was used in our scenarios, we found that covariance had negligible effects on the stochastic growth rate of slow-living populations, indicating a large degree of buffering in these species. For fast-living species, covariance had contrasting effects on the stochastic dynamics. These effects were strengthened by harsher relationships between the vital rates and the environmental driver (i.e., using a log-log link function). Collectively, these findings strengthen the importance of characterising concurrent changes in the mean, variance and covariance of vital rates to explicit environmental drivers to predict population responses to environmental variability, especially among fast life histories.

Demographic lability along the fast-slow continuum

The set of demographic lability with forced buffering scenarios tested have yielded insights into the demographic strategies in variable environments along the fast-slow continuum for a range of animal life histories. While different assumptions have been made as to which vital rates should be labile (Hilde *et al.*, 2020; McDonald *et al.*, 2017), we found that demographic lability among the least ($f_j(z)$ and/or $s_{immature}(z)$) or the most ($s_{mature}(z)$) influential vital rates is likely an adaptive response to changes in environmental variance for many fast-living life histories.

However, positive effects of variability on $\ln(\lambda_s)$ were stronger and more prevalent with lability in both fertility and survival of the non-reproductive stages (the most influential). These results emphasize that both fertility and survival rates can exhibit convex responses to environmental variability in these populations, and yield positive effects on $\ln(\lambda_s)$ when the combination of all vital rates with different curvatures reduced σ^2_λ. In contrast, among populations of slow-living life histories, lability among the most influential vital rates led to negative effects of increased environmental variance on $\ln(\lambda_s)$. Selection for a reduction in temporal variation of the vital rates that contribute the most to population growth combined with other rates varying more freely, as stated by the demographic buffering hypothesis, seems therefore more likely among slow-living species with a similar life history as in our analysis.

Labile and buffered vital rates in our scenarios were assigned based on general expectations along the fast-slow continuum. These assumptions, while accurate for some life histories, may be different for other populations with the same generation time. For instance, young and old adult survival probabilities may respond differently to variation. Further insights would require differentiating labile and buffered (st)age-specific vital rates in a population based on each rate's sensitivity.

Overall, this study emphasizes the importance of considering explicit links between vital rates and environmental drivers as well as the covariance structure of vital rates, in order to quantify long-term fitness effects of environmental variability. Across the fast-slow continuum of animal life histories, faster-living species have the largest potential for using demographic lability as an adaptive response to variability, while demographic buffering seems to be the main adaptive response in slow-living species. These findings have important implications for predicting population and species responses to changes in environmental variance under climate change.

References

Altwegg, R., Schaub, M. & Roulin, A. (2007). Age-specific fitness components and their temporal variation in the barn owl. *Am. Nat.*, 169, 47–61.

Barraquand, F. & Yoccoz, N.G. (2013). When can environmental variability benefit population growth? Counterintuitive effects of nonlinearities in vital rates. *Theor. Popul. Biol.*, 89, 1–11.

Boyce, M., Haridas, C., Lee, C. & NCEAS Stochastic Demography Working Group (2006). Demography in an increasingly variable world. *Trends Ecol. Evol.*, 21, 141–148.

Caswell, H. (2001). *Matrix Population Models: Construction, Analysis, and Interpretation.* 2nd edn.

Clark, T.J. & Luis, A.D. (2020). Nonlinear population dynamics are ubiquitous in animals. *Nat. Ecol. Evol*, 4, 75–81.

Colchero, F., Jones, O., Conde, D.A., Hodgson, D., Zajitschek, F., Schmidt, B.R. *et al.* (2019). The diversity of population responses to environmental change. *Ecol. Lett.*, 22, 342–353.

Compagnoni, A., Bibian, A.J., Ochocki, B.M., Rogers, H.S., Schultz, E.L., Sneck, M.E. *et al.* (2016). The effect of demographic correlations on the stochastic population dynamics of perennial plants. *Ecol. Monogr.*, 86, 480–494.

Compagnoni, A., Levin, S., Childs, D.Z., Harpole, S., Paniw, M., Römer, G. *et al.* (2021). Herbaceous perennial plants with short generation time have stronger responses to climate anomalies than those with longer generation time. *Nat. Commun.*, 12, 1–8.

Coulson, T., Gaillard, J.M. & Festa-Bianchet, M. (2005). Decomposing the variation in population growth into contributions from multiple demographic rates. *J. Anim. Ecol.*, 74, 789–801.

Dahlgren, D.K., Guttery, M.R., Messmer, T.A., Caudill, D., Dwayne Elmore, R., Chi, R. *et al.* (2016). Evaluating vital rate contributions to greater sage-grouse population dynamics to inform conservation. *Ecosphere*, 7, 1–15.

Dahlgren, J.P., García, M.B. & Ehrlén, J. (2011). Nonlinear relationships between vital rates and state variables in demographic models. *Ecology*, 92, 1181–1187.

Dalgleish, H.J., Koons, D.N. & Adler, P.B. (2010). Can life-history traits predict the response of forb populations to changes in climate variability? *J. Ecol.*, 98, 209–217.

Doak, D.F., Morris, W.F., Pfister, C., Kendall, B.E. & Bruna, E.M. (2005). Correctly estimating how environmental stochasticity influences fitness and population growth. *Am. Nat.*, 166, E14–E21.

Drake, J.M. (2005). Population effects of increased climate variation. *Proc. R. Soc. Lond. B Biol. Sci.*, 272, 1823–1827.

Engen, S., Lande, R., Sæther, B.E. & Dobson, S.F. (2009). Reproductive value and the stochastic demography of age-structured populations. *Am. Nat.*, 174, 795–804.

Gaillard, J.M., Lemaitre, J.F., Berger, V., Bonenfant, C., Devillard, S., Douhard, M. *et al.* (2016). Axes of variation in life histories. In: *Encyclopedia of Evolutionary Biology.* Academic Press, Oxford, pp. 312–323. Kliman r.m. edn.

Gaillard, J.M. & Yoccoz, N.G. (2003). Temporal variation in survival of mammals: a case of environmental canalization? *Ecology*, 84, 3294–3306.

Gaillard, J.M., Yoccoz, N.G., Lebreton, J.D., Bonenfant, C., Devillard, S., Loison, A. *et al.* (2005). Generation time: a reliable metric to measure life-history variation among mammalian populations. *Am. Nat.*, 166, 119–123.

Gill, J. (2001). *Generalized Linear Models: A Unified Approach.* Thousand Oaks, CA: Sage.

Hansen, E.S., Sandvik, H., Erikstad, K.E., Yoccoz, N.G., Anker-Nilssen, T., Bader, J. *et al.* (2021). Centennial relationships between ocean temperature and Atlantic puffin production reveal shifting decennial trends. *Glob. Chang. Biol.*, 27, 3753–3764.

Henden, J.A., Bårdsen, B.J., Yoccoz, N.G. & Ims, R.A. (2008). Impacts of differential prey dynamics on the potential recovery of endangered arctic fox populations. *J. Appl. Ecol.*, 45, 1086–1093.

Hilde, C.H., Gamelon, M., Sæther, B.E., Gaillard, J.M., Yoccoz, N.G. & Pélabon, C. (2020). The Demographic Buffering Hypothesis: Evidence and Challenges. *Trends. Ecol. Evol.*, 35, 523–538.

Huntingford, C., Jones, P.D., Livina, V.N., Lenton, T.M. & Cox, P.M. (2013). No increase in global temperature variability despite changing regional patterns. *Nature*, 500, 327–330.

Iles, D.T., Rockwell, R.F. & Koons, D.N. (2019). Shifting Vital Rate Correlations Alter Predicted Population Responses to Increasingly Variable Environments. *Am. Nat.*, 193, E57–E64.

IPCC (2021). The Physical Science Basis. Contribution of Working Group I to the Sixth Assessment Report of the Intergovernmental Panel on Climate Change[Masson-Delmotte, V., P. Zhai, A. Pirani, S. L. Connors, C. Péan, S. Berger, N. Caud, Y. Chen, L. Goldfarb, M. I. Go. Tech. rep., Cambridge University Press. In Press.

Jenouvrier, S., Holland, M., Stroeve, J., Barbraud, C., Weimerskirch, H., Serreze, M. *et al.* (2012). Effects of climate change on an emperor penguin population: Analysis of coupled demographic and climate models. *Glob. Chang. Biol.*, 18, 2756–2770.

Johnson, H.E., Mills, L.S., Stephenson, T.R. & Wehausen, J.D. (2010). Population-specific vital rate contributions influence management of an endangered ungulate. *Ecol. Appl.*, 20, 1753–1765.

Jongejans, E., de Kroon, H., Tuljapurkar, S. & Shea, K. (2010). Plant populations track rather than buffer climate fluctuations. *Ecol. Lett.*, 13, 736–743.

Koons, D.N., Pavard, S., Baudisch, A. & Metcalf, C.J.E. (2009). Is life-history buffering or lability adaptive in stochastic environments? *Oikos*, 118, 972–980.

Kotz, M., Wenz, L. & Levermann, A. (2021). Footprint of greenhouse forcing in daily temperature variability. *Proc. Natl. Acad. Sci. U.S.A.*, 118, 1–8.

Lande, R., Engen, S. & Saether, B.E. (2003). *Stochastic population dynamics in ecology and conservation.* Oxford University Press, Oxford.

Laufkötter, C., Zscheischler, J. & Frölicher, T.L. (2020). High-impact marine heatwaves attributable to human-induced global warming. *Science*, 369, 1621–1625.

Lawson, C.R., Vindenes, Y., Bailey, L. & van de Pol, M. (2015). Environmental variation and population responses to global change. *Ecol. Lett.*, 18, 724–736.

Le Coeur, C., Storkey, J. & Ramula, S. (2021). Population responses to observed climate variability across multiple organismal groups. *Oikos*, 130, 476–487.

Lewontin, R.C. & Cohen, D. (1969). On population growth in a randomly varying environment. *Proc. Natl. Acad. Sci. U.S.A.*, 62, 1056–1060.

Louthan, A.M. & Morris, W. (2021). Climate change impacts on population growth across a species' range differ due to nonlinear responses of populations to climate and variation in rates of climate change. *PLoS ONE*, 16, e0247290.

McDonald, J.L., Franco, M., Townley, S., Ezard, T.H., Jelbert, K. & Hodgson, D.J. (2017). Divergent demographic strategies of plants in variable environments. *Nat. Ecol. Evol*, 1, 0029.

Morris, W.F., Pfister, C.A., Tuljapurkar, S., Haridas, C., Boggs, C., Boyce, M. *et al.* (2008). Longevity can buffer plant and animal populations against changing climate variability. *Ecology*, 89, 19–25.

Mysterud, A., Stenseth, N.C., Yoccoz, N.G., Langvatn, R. & Steinheim, G. (2001). Nonlinear effects of large-scale climatic variability on wild and domestic herbivores. *Nature*, 410, 1096–1099.

Paniw, M., Ozgul, A. & Salguero-Gómez, R. (2018). Interactive life-history traits predict sensitivity of plants and animals to temporal autocorrelation. *Ecol. Lett.*, 21, 275–286.

Pendergrass, A.G., Knutti, R., Lehner, F., Deser, C. & Sanderson, B.M. (2017). Precipitation variability increases in a warmer climate. *Sci. Rep.*, 7, 17966.

Pfister, C.A. (1998). Patterns of variance in stage-structured populations: Evolutionary predictions and ecological implications. *Proc. Natl. Acad. Sci. U.S.A.*, 95, 213–218.

van de Pol, M., Vindenes, Y., Saether, B.E., Engen, S., Ens, B.J., Oosterbeek, K. *et al.* (2010). Effects of climate change and variability on population dynamics in a long-lived shorebird. *Ecology*, 91, 1192–1204.

R Core Team (2020). R: A language and environment for statistical computing.

Rotella, J.J., Link, W.A., Chambert, T., Stauffer, G.E. & Garrott, R.A. (2012). Evaluating the demographic buffering hypothesis with vital rates estimated for Weddell seals from 30 years of mark-recapture data. *J. Anim. Ecol.*, 81, 162–173.

Ruel, J.J. & Ayres, M.P. (1999). Jensen's inequality predicts effects of environmental variation. *Trends Ecol. Evol.*, 14, 361–366.

Salguero-Gómez, R. (2021). Commentary on the life history special issue: The fast-slow continuum is not the end-game of life history evolution, human or otherwise. *Evol. Hum. Behav.*, 42, 281–283.

Salguero-Gómez, R., Jones, O.R., Archer, C.R., Bein, C., de Buhr, H., Farack, C. *et al.* (2016a). COMADRE: A global data base of animal demography. *J. Anim. Ecol.*, 85, 371–384.

Salguero-Gómez, R., Jones, O.R., Jongejans, E., Blomberg, S.P., Hodgson, D.J., Mbeau-Ache, C. *et al.* (2016b). Fast–slow continuum and reproductive strategies structure plant life-history variation worldwide. *Proc. Natl Acad. Sci.*, 113, 230–235.

Santos, G.S., Salguero-Gómez, R., Dias, A.T.C. & Kajin, M. (2021). To buffer or to be labile? A framework to disentangle demographic patterns and evolutionary processes. *bioRxiv.*

Stearns, S.C. (1989). Trade-offs in life-history evolution. *Funct. Ecol.*, 3, 259–268.

Stearns, S.C. (1992). *The evolution of life histories.* Oxford University Press, New York.

Tuljapurkar, S. (1982). Population dynamics in variable environments. III. Evolutionary dynamics of r-selection. *Theor. Popul. Biol.*, 21, 141–165.

Tuljapurkar, S. (1990). *Population Dynamics in Variable Environments.* Springer-Verlag, NewYork.

Tuljapurkar, S. & Orzack, S.H. (1980). Population dynamics in variable environments I. Long-run growth rates and extinction. *Theor. Popul. Biol.*, 18, 314–342.

Text box 1: Glossary

Demographic lability or labile vital rate: A labile vital rate fluctuates with temporal variation in environmental conditions. The relationship between a labile vital rate and the environment (e.g., a key environmental driver) can be convex, concave or linear, so that the average value of this vital rate in a variable environment becomes $>$, $<$, or $=$ to the vital rate estimated in the mean environment (z=0), respectively.

Adaptive demographic lability (demographic lability hypothesis): selection for vital rates to track environmental fluctuations that leads to an overall increased long-term fitness, $ln(\lambda_s)$. Increase in $ln(\lambda_s)$ occurs when an increase in the vital rate means due to convexity in the vital rate responses leads to a shift in the arithmetic mean of annual population growth rates $ln(\bar{\lambda})$, that overcomes the detrimental effect of temporal variance in the annual population growth rates σ^2. This hypothesis relies on the assumption that some labile vital rates are convex functions of the environment or more precisely, that the demographic lability index is positive.

Demographic lability index (DLI): The DLI (Equation 1) indicates the total effect of lability on the arithmetic mean of annual growth rates due to environmental variability $\Delta ln(\bar{\lambda})$ for a given life history. This index corresponds to the sum over all (st)ages of the second derivatives of survival and fertility at the mean environment (z=0), weighted by the sensitivity of λ_0 to the corresponding vital rate. When positive (/negative), the DLI is an indicator of adaptive (/non adaptive) lability through overall positive (/negative) contribution from convexity (/concavity) of the vital rates. Adaptive lability can lead to a positive overall effect of environmental variability on long-term fitness $ln(\lambda_s)$ when increases of $ln(\bar{\lambda})$ overcome the detrimental effect of increased σ^2 (see Equation 1).

Demographic buffering or buffered vital rate: Reduced variation of a vital rate in response to temporal variation in the environmental variable z. A more flat relationship between the vital rate and the environment z leads to lower vital rate variance, and the mean vital rate in a variable environment remains approximately equal to vital rate in the mean environment (z=0).

Adaptive demographic buffering (demographic buffering hypothesis): prediction that natural selection should favour a reduction in variance of the vital rates with the strongest influence on long-term fitness, reducing the temporal variance in annual population growth rates σ^2 and leading to an overall stable or increased fitness in variable environments. This hypothesis relies on the assumption that $ln(\bar{\lambda})$ is not affected by environmental variance ($ln(\lambda_0) \approx ln(\bar{\lambda})$), which thereby assume low variation or linear vital rate responses to environmental variability.

Text box 2: Tuljapurkar's approximation: effects of vital rate mean, variance and covariance on long-term fitness

The 'small-noise' approximation of Tuljapurkar (1982) for an environment with no autocorrelation is given by:

$$ln\lambda_s \approx ln\bar{\lambda} - \frac{\sigma_\lambda^2}{2\bar{\lambda}^2} \tag{2}$$

where

$$\sigma_\lambda^2 = \sum_{ijkl} \frac{d\bar{\lambda}}{da_{ij}} \frac{d\bar{\lambda}}{da_{kl}} Cov(a_{ij}, a_{kl}). \tag{3}$$

Here, $\bar{\lambda}$ is the dominant eigenvalue of the average matrix across variable environments $\bar{\mathbf{A}}$ and σ_λ^2 is the variance of the annual population growth rate caused by temporal variance and covariance in the matrix elements (vital rates in age structured populations; Equation 3). In equation (3), a_{ij} refers to element i, j of the average matrix $\bar{\mathbf{A}}$, $\frac{d\bar{\lambda}}{da_{ij}}$ is the sensitivity of $\bar{\lambda}$ to changes in a_{ij} and $Cov(a_{ij}, a_{kl})$ corresponds to the covariance between matrix elements a_{ij} and a_{kl}.

Based on this approximation, increases in the variance of the different matrix elements and/or positive covariance between them in a variable environment reduce $ln(\lambda_s)$ by increasing the variance in annual population growth rates (σ_λ^2). Under the assumption of small fluctuations in the vital rates (i.e., weak relationships with environment), $ln(\bar{\lambda})$ would equal $ln(\lambda_0)$, where λ_0 is the dominant eigenvalue of the projection matrix for the constant environment.

However, in case of nonlinear vital rate responses to environmental variability, not only the variance, but also the mean of vital rates can change and thereby change the arithmetic mean $\bar{\lambda}$. The resulting change in $ln(\bar{\lambda})$ is a measure of the effects of demographic lability for a given life history (positive, negative or null). Effects on $ln(\bar{\lambda})$ are positive if at least some vital rates show convex relationships with the environment; negative if some vital rates are concave functions of the environment; and null if the vital rate responses are linear or if concave/convex responses are weak or cancel each other out.

Although simulations in our study were not limited to small fluctuations in the vital rates, the two sides of equation (2) were found to be approximately equal (Supporting information 5).

Figure captions

Figure 1. Simulation framework for studying the effect of increased environmental variability on long-term fitness (measured by the stochastic population growth rate $ln(\lambda_s)$). **A.** From each matrix population model (N_{tot}= 81), (st)age-specific survival rates $s_j(z)$ and fertilities $f_j(z)$ were extracted and perturbed through time following nonlinear relationships with an environmental driver z (independent and identically distributed variable, z $\sim \mathcal{N}(0,1)$). A low (β_z= 0.1) and high (β_z= 0.5) environmental variability scenarios were considered. Based on 4000 stochastic simulations of 200 time steps each, the difference in $ln(\lambda_s)$ between the two scenarios, referred to as $\Delta ln(\lambda_s)$, was estimated and decomposed into changes in the arithmetic mean $\Delta ln(\bar{\lambda})$ and in the temporal variance of the annual population growth rates $\Delta\sigma^2$. **B.** Two or three different link-functions were considered for $s_j(z)$ and $f_j(z)$, respectively. **C. Scenarios 1-8:** Four combinations were examined including logistic functions for all vital rates, log-log link functions for all vital rates and two combinations of exponential fertilities $f_j(z)$ (log link) with logistic or log-log link function for $s_j(z)$. These four combinations were tested with positive or negative covariance between survival and fertility. **Scenarios 9-11:** Scenarios of demographic lability among the (st)age-specific fertility coefficients or among the fertility coefficients and survival rates of the non-reproductive stages ($S_{immature}$). **Scenarios 12-13:** Scenarios of demographic lability among the (st)age-specific $s_j(z)$ or among the survival rates of the reproductive stages only (S_{mature}). Labile vital rates were logistic functions of z while the other rates were held constant and fixed to the values reported in the COMADRE projection matrix (forced buffering).

Figure 2. Mid panels: Change in long-term fitness ($\Delta ln(\lambda_s)$) due to increased environmental variability across generation time, under four scenarios of covariance and link-functions of the vital rates (scenarios 1-8, Fig. 1). The four scenarios are illustrated on the left panel, with the grey and black lines corresponding to the (st)age-specific survival rates $s_j(z)$ and fertility coefficients $f_j(z)$, respectively (functions varied for each stage depending on $s_j(0)$ and $f_j(0)$; only one function is shown for survival and fertility here). For each population, positive (panels a-b) and negative (panels c-d) covariance between $f_j(z)$ and $s_j(z)$ were simulated, considering $f_j(z)$ and $s_j(z)$ as logistic functions (panels a-c) or log-log link functions (panels b-d) of the environment z. Panels to the right show the decomposition of $\Delta ln(\lambda_s)$ into changes in the arithmetic mean $\Delta ln(\bar{\lambda})$ (y-axis) and variance $\Delta\sigma^2$ (x-axis). Colors refer to the demographic lability index: Positive (red) and negative (blue) values indicate populations with overall convexity or concavity, respectively, of their (st)age-specific vital rates with z.

Figure 3. Mid panels: Change in long-term fitness ($\Delta ln(\lambda_s)$) due to increased environmental variability across generation time using logistic (panels a-c) or log-log (panels b-d) link functions for (st)age-specific survival rates, and log link function for fertilities (scenarios 1-8, Fig. 1). For each population, positive (panels a-b) and negative (panels c-d) covariance between (st)age-specific survival rates $s_j(z)$ and fertilities $f_j(z)$ were simulated. Panels to the right show the decomposition of $\Delta ln(\lambda_s)$ into changes in the arithmetic mean $\Delta ln(\bar{\lambda})$ (y-axis) and variance $\Delta\sigma^2$ (x-axis). Colors refer to the demographic lability index: Positive (red) and negative (blue) values indicate populations with overall convexity or concavity, respectively, of their (st)age-specific vital rates with z.

Figure 4. Results from scenarios of forced buffering with demographic lability among (a) (st)age-specific survival rates, (b) survival rates of the reproductive stages only, (c) (st)age-specific fertilities and (d-e) fertilities and survival rates of the non-reproductive stages. For each scenario, the change in $ln(\lambda_s)$ between high (β_z= 0.5) and low (β_z= 0.1) environmental variability simulated for each population was plotted against generation time (mid panels). Labile vital rates were logistic functions of the environment z, while other rates were held constant and fixed to the values reported in the COMADRE projection matrix. Same legend as Figure 2 and 3.

Figure 1.

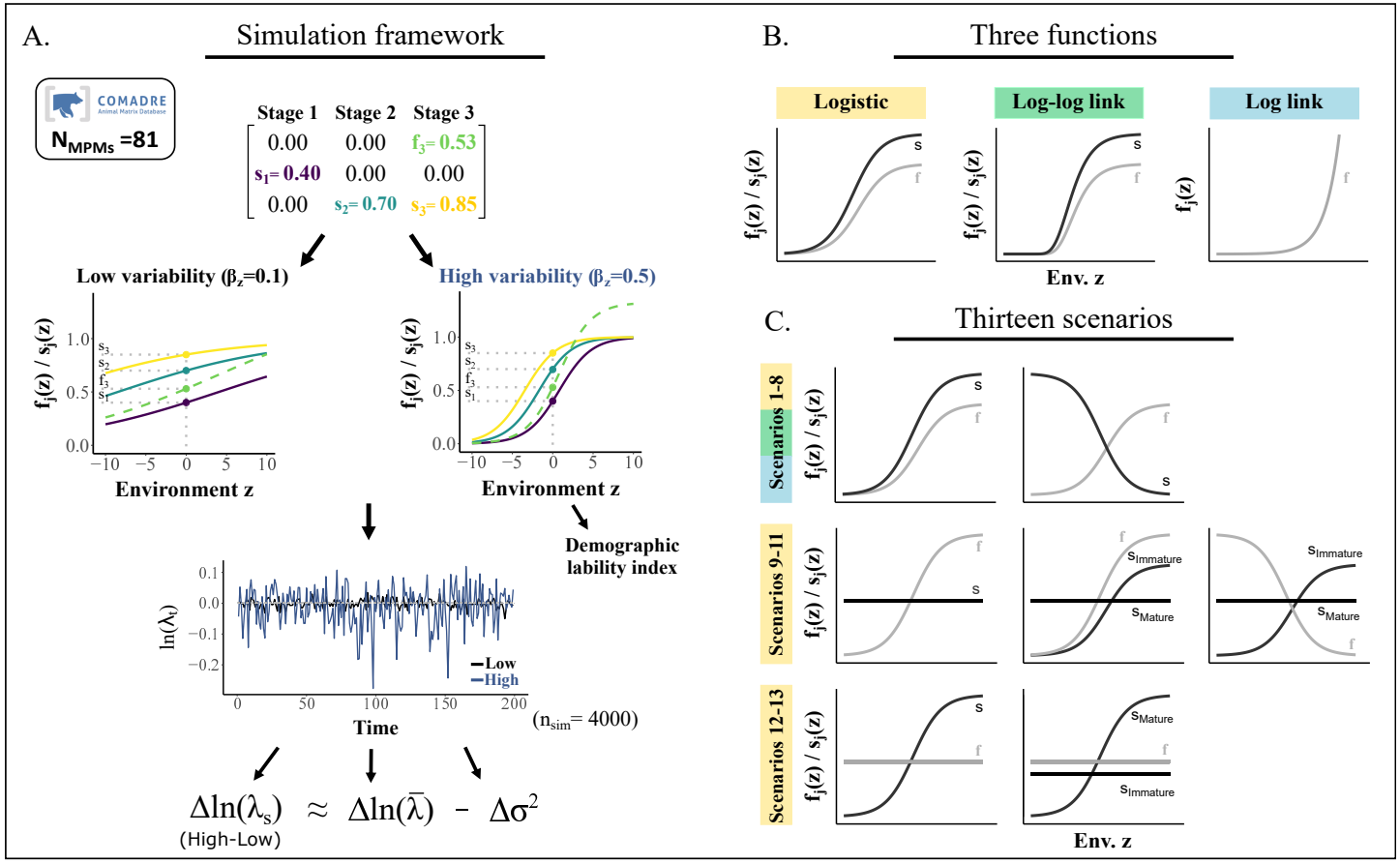
A.
Simulation framework
COMADRE
Animal Matrix Database
N_MPMs =81
Stage 1 Stage 2 Stage 3
0.00 0.00 f3= 0.53
s1= 0.40 0.00 0.00
0.00 s2= 0.70 s3= 0.85
Low variability (βz=0.1)
High variability (βz=0.5)
fj(z) / sj(z)
Environment z
Demographic lability index
ln(λt)
Time
Low
High
(nsim= 4000)
Δln(λs) ≈ Δln(λ̄) - Δσ2
(High-Low)
B.
Three functions
Logistic
Log-log link
Log link
fj(z) / sj(z)
fj(z)
Env. z
C.
Thirteen scenarios
Scenarios 1-8
Scenarios 9-11
Scenarios 12-13
sImmature
sMature
Env. z

Figure 2.

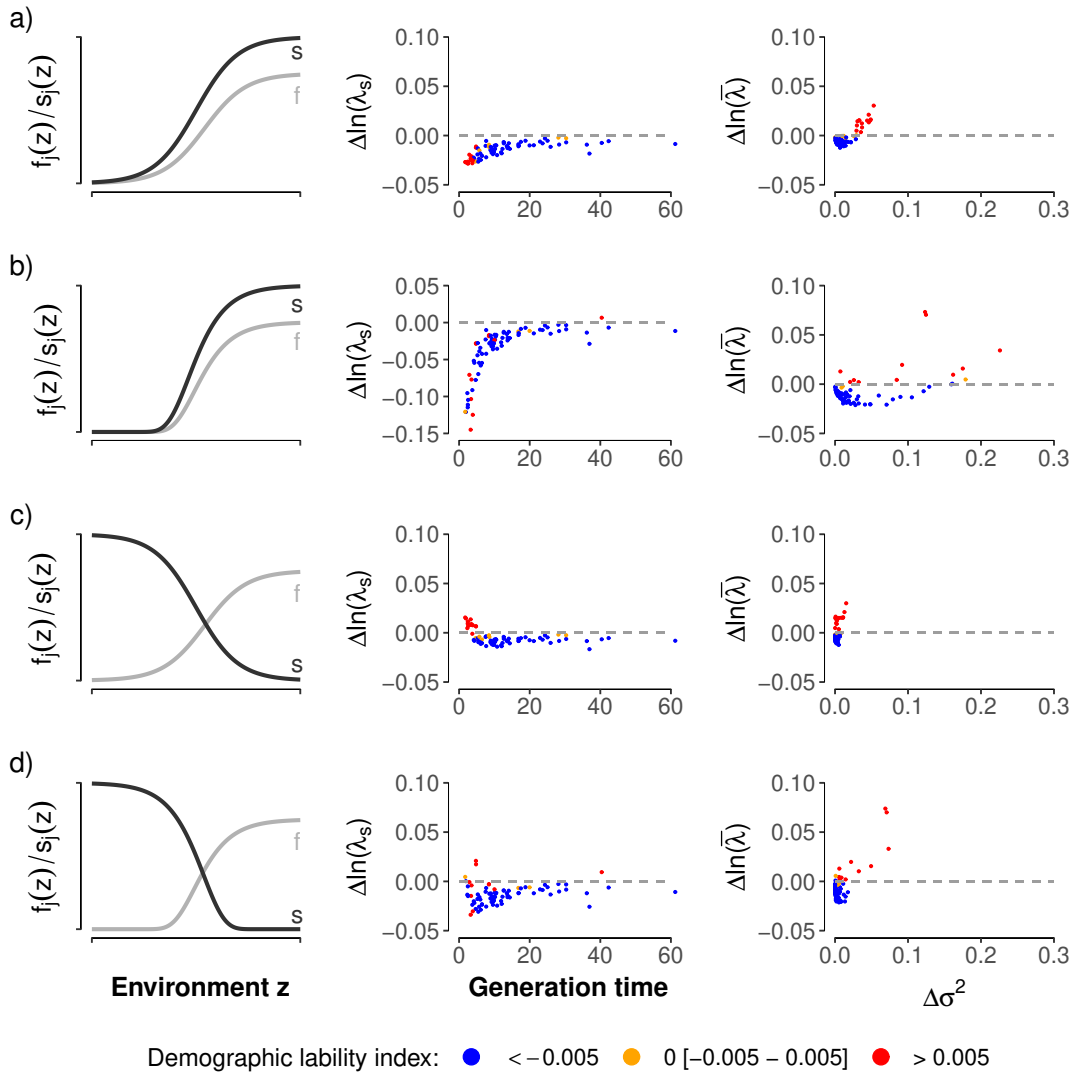
a)
b)
c)
d)
$f_j(z)/s_j(z)$
s
f
$\Delta\ln(\lambda_s)$
$\Delta\ln(\bar{\lambda})$
0.10
0.05
0.00
−0.05
−0.10
−0.15
0
20
40
60
0.0
0.1
0.2
0.3
Environment z
Generation time
$\Delta\sigma^2$
Demographic lability index:
< −0.005
0 [−0.005 – 0.005]
> 0.005

Figure 3.

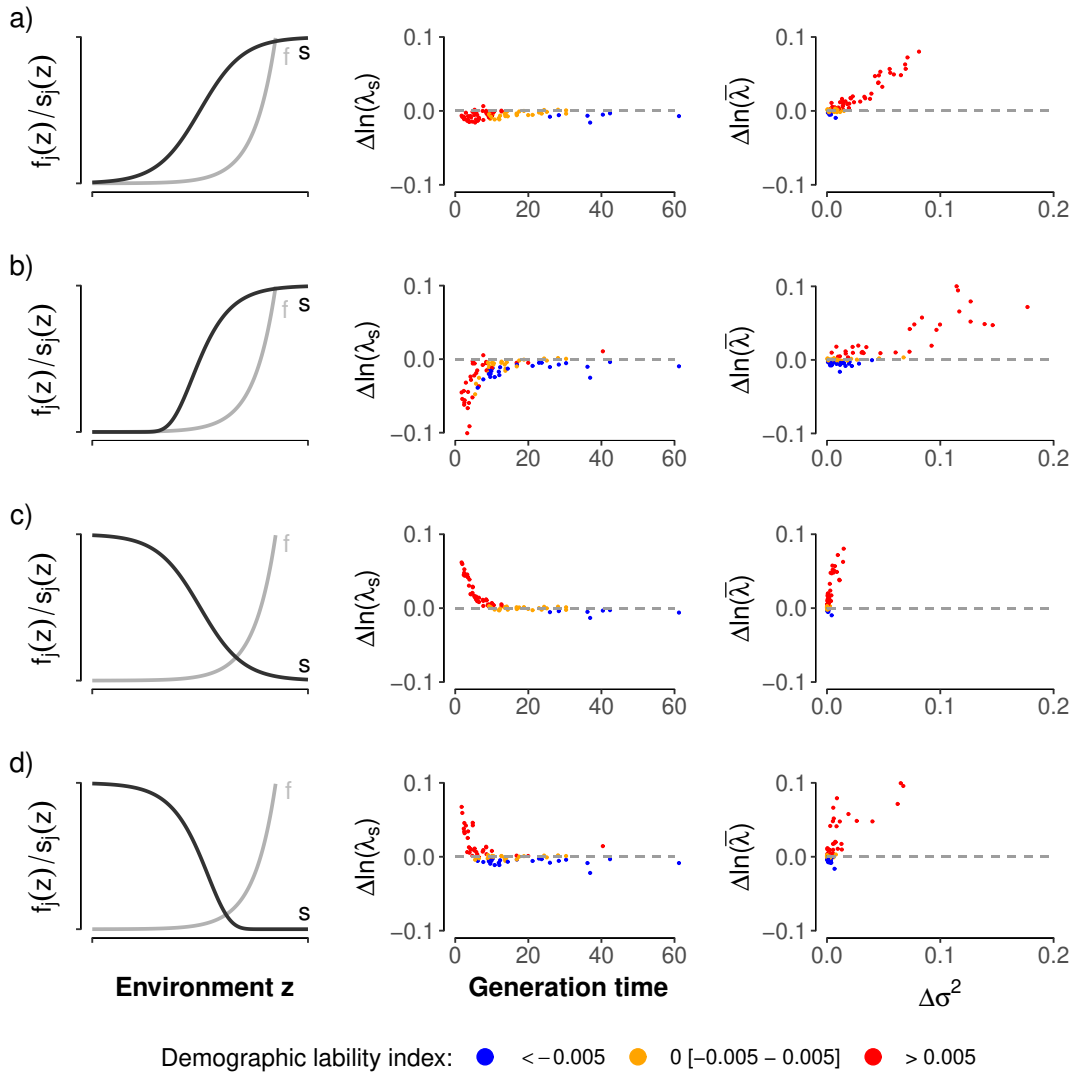
a)
b)
c)
d)
$f_j(z)/s_j(z)$
f
s
$\Delta\ln(\lambda_s)$
$\Delta\ln(\bar{\lambda})$
0.1
0.0
−0.1
0
20
40
60
0.0
0.1
0.2
Environment z
Generation time
$\Delta\sigma^2$
Demographic lability index:
< −0.005
0 [−0.005 – 0.005]
> 0.005

Figure 4.

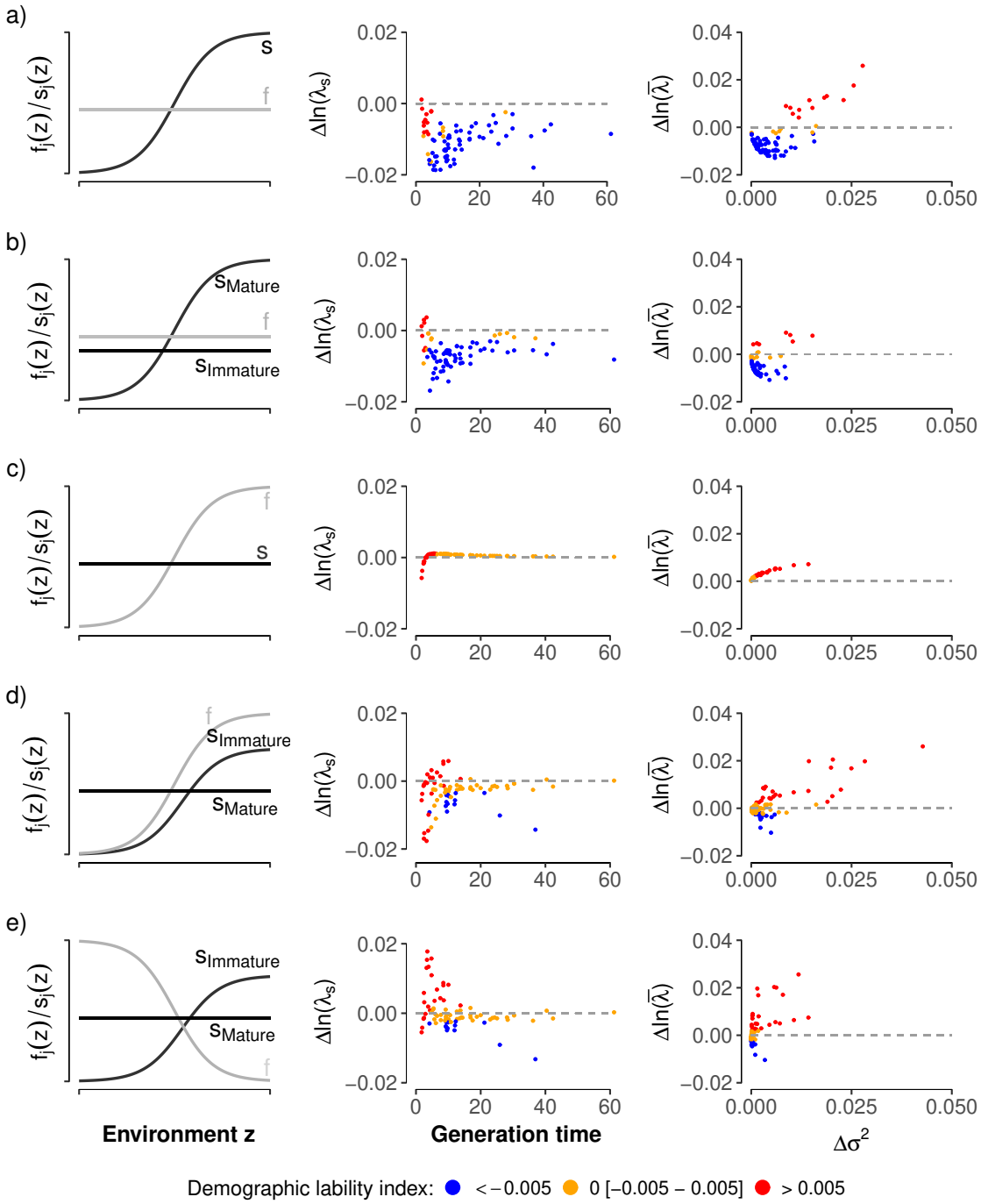
a)
b)
c)
d)
e)
$f_j(z)/s_j(z)$
s
f
s_{Mature}
$s_{Immature}$
$\Delta\ln(\lambda_s)$
$\Delta\ln(\bar{\lambda})$
0.02
0.00
−0.02
0.04
0
20
40
60
0.000
0.025
0.050
Environment z
Generation time
$\Delta\sigma^2$
Demographic lability index: < −0.005 0 [−0.005 – 0.005] > 0.005